AIP Journal of Applied Physics

Indirect monitoring shot-to-shot shock waves strength reproducibility during pump–probe experiments

T. A. Pikuz, A. Ya. Faenov, N. Ozaki, N. J. Hartley, B. Albertazzi, T. Matsuoka, K. Takahashi, H. Habara, Y. Tange, S. Matsuyama, K. Yamauchi, R. Ochante, K. Sueda, O. Sakata, T. Sekine, T. Sato, Y. Umeda, Y. Inubushi, T. Yabuuchi, T. Togashi, T. Katayama, M. Yabashi, M. Harmand, G. Morard, M. Koenig, V. Zhakhovsky, N. Inogamov, A. S. Safronova, A. Stafford, I. Yu. Skobelev, S. A. Pikuz, T. Okuchi, Y. Seto, K. A. Tanaka, T. Ishikawa, and R. Kodama

Citation: Journal of Applied Physics **120**, 035901 (2016); doi: 10.1063/1.4958796
View online: http://dx.doi.org/10.1063/1.4958796
View Table of Contents: http://scitation.aip.org/content/aip/journal/jap/120/3?ver=pdfcov
Published by the AIP Publishing

Indirect monitoring shot-to-shot shock waves strength reproducibility during pump–probe experiments

T. A. Pikuz,[1,2,3,a)] A. Ya. Faenov,[3,4] N. Ozaki,[1,2] N. J. Hartley,[4] B. Albertazzi,[1] T. Matsuoka,[4] K. Takahashi,[2] H. Habara,[1,2] Y. Tange,[5] S. Matsuyama,[1] K. Yamauchi,[1] R. Ochante,[1] K. Sueda,[2] O. Sakata,[6] T. Sekine,[7] T. Sato,[7] Y. Umeda,[7] Y. Inubushi,[5,8] T. Yabuuchi,[8] T. Togashi,[5,8] T. Katayama,[5,8] M. Yabashi,[5,8] M. Harmand,[9] G. Morard,[9] M. Koenig,[4,10] V. Zhakhovsky,[11] N. Inogamov,[12] A. S. Safronova,[13] A. Stafford,[13] I. Yu. Skobelev,[3,14] S. A. Pikuz,[3,14] T. Okuchi,[15] Y. Seto,[16] K. A. Tanaka,[1,2] T. Ishikawa,[8] and R. Kodama[1,2]
[1]*Graduate School of Engineering, Osaka University, Suita, Osaka 565-0871 Japan*
[2]*Photon Pioneers Center, Osaka University, Suita, Osaka 565-0871 Japan*
[3]*Joint Institute for High Temperatures, Russian Academy of Sciences, Moscow 125412, Russia*
[4]*Institute for Academic Initiatives, Osaka University, Suita, Osaka 565-0871, Japan*
[5]*Japan Synchrotron Radiation Research Institute, Sayo, Hyogo 679-5198, Japan*
[6]*Synchrotron X-ray Station at SPring-8, NIMS, Sayo, Hyogo 679-5148, Japan*
[7]*Graduate School of Science, Hiroshima University, Higashi-Hiroshima 739-8526, Japan*
[8]*RIKEN Spring-8 Center, Sayo, Hyogo 679-5148 Japan*
[9]*IMPMC, Université Pierre et Marie Curie, CNRS, 75005 Paris, France*
[10]*LULI - CNRS, Ecole Polytechnique, CEA: Université Paris-Saclay, UPMC Univ Paris 06: Sorbonne Universités, F-91128 Palaiseau Cedex, France*
[11]*All-Russia Research Institute of Automatics, ROSATOM, Moscow 127055, Russia*
[12]*L. D. Landau Institute for Theoretical Physics, Russian Academy of Science, Chernogolovka 142432, Russia*
[13]*Physics Department, University of Nevada, Reno, Nevada 89557, USA*
[14]*National Research Nuclear University MEPhI, Moscow 115409, Russia*
[15]*Institute for Planetary Materials, Okayama University, Touhaku, Tottori 682-0193, Japan*
[16]*Graduate School of Science, Kobe University, Kobe 657-8501, Japan*

(Received 5 April 2016; accepted 1 July 2016; published online 18 July 2016)

We present an *indirect* method of estimating the strength of a shock wave, allowing *on line* monitoring of its reproducibility in each laser shot. This method is based on a shot-to-shot measurement of the X-ray emission from the ablated plasma by a high resolution, spatially resolved focusing spectrometer. An optical pump laser with energy of 1.0 J and pulse duration of ~660 ps was used to irradiate solid targets or foils with various thicknesses containing Oxygen, Aluminum, Iron, and Tantalum. The high sensitivity and resolving power of the X-ray spectrometer allowed spectra to be obtained on each laser shot and to control fluctuations of the spectral intensity emitted by different plasmas with an accuracy of ~2%, implying an accuracy in the derived electron plasma temperature of 5%–10% in pump–probe high energy density science experiments. At nano- and sub-nanosecond duration of laser pulse with relatively low laser intensities and ratio Z/A ~ 0.5, the electron temperature follows $T_e \sim I_{las}^{2/3}$. Thus, measurements of the electron plasma temperature allow *indirect* estimation of the laser flux on the target and control its shot-to-shot fluctuation. Knowing the laser flux intensity and its fluctuation gives us the possibility of monitoring shot-to-shot reproducibility of shock wave strength generation with high accuracy. *Published by AIP Publishing*. [http://dx.doi.org/10.1063/1.4958796]

I. INTRODUCTION

The properties and behavior of matter at extreme conditions are increasingly important for fundamental physics and applications.[1] High energy lasers have allowed experiments to reach greater pressures than that are possible with techniques such as diamond anvil cells and gas gun projectile impacts.[2,3] By rapidly ablating the surface of a sample, or of an ablator layer designed for this purpose, strong shocks can be driven into the sample.

Typically, sub-nanosecond or nanosecond laser pulses with intensities 10^{11}–10^{13} W/cm^2 are used as generators of shock waves, driving pressures up to hundreds of GPa in condensed matter (see, for example, Refs. 4–7). Now, with available laser intensities on the target up to 10^{15} W/cm^2, reaching pressures of multiple TPa[8] starts to be possible. Better understanding of material properties under such conditions is of great interest in different fields including inertial fusion energy research, planetary formation, and science.

Recent advances in ultrafast pump-probe experiments, notably with X-ray Free Electron Lasers (XFELs), have allowed *in situ* studies of matter deformation, melting, and ablation at the lattice-level for the first time.[9,10] Although driving with high intensity lasers is capable of reaching the highest pressure conditions currently possible in laboratory experiments, it suffers from a lack of shot-to-shot reproducibility due to the variation in the laser energy, target quality, and focusing stability.

a)Email: tatiana.pikuz@eie.eng.osaka-u.ac.jp

In this regard, the question arises as to what level of shot-to-shot reproducibility of the shock wave amplitude can be achieved in a given laser system. It is necessary to underline that diagnosing the strength of the shock, and consequently the conditions reached in the sample, is often difficult and no direct measurement methods have been developed yet. To address this, we present an *indirect* technique, which enables estimation of the shock wave strength and allows *on line* monitoring of its shot-to-shot reproducibility. It is based on measurements of the X-ray emission spectra, which are used to determine the electron plasma temperature reached in the ablated plasma. This allows us to estimate the laser intensity on the target surface and, knowing that, to *indirectly* calculate the pressure of the shock wave from empirically derived relationships. Using such an approach, we show that, on the one hand, laser-produced plasma in the case of reproducible laser and target operations could be a stable source of X-ray radiation, and on the other hand, high-resolution X-ray spectroscopy is an effective *indirect* diagnostic of the pressure value reached in the sample and its shot-to-shot reproducibility.

As was shown in Ref. 5, for laser pulses with nano and sub-nanosecond durations, the electron temperature T_e in samples with a ratio of atomic number (Z) to atomic weight (A) Z/A $\sim$ 1/2 is directly related to the laser intensity I_L as

$$T_e[\mathrm{keV}] \sim 13.7(I_L[10^{15}\,\mathrm{W\,cm^{-2}}]\lambda^2[\mu\mathrm{m}])^{2/3}, \qquad (1)$$

where λ is the wavelengths of laser irradiation. Using this, and knowing the electron temperature of the plasma, we are able to evaluate the incident laser intensity I_L.

In such case for Z/A $\sim$ 1/2, the ablation pressure

$$P_a[\mathrm{Mbar}] \sim 57\left\{\frac{I_L[10^{15}\,\mathrm{W\,cm^{-2}}]}{(\lambda[\mu\mathrm{m}])^{\frac{2}{3}}}\right\}^{2/3}, \qquad (2)$$

is also related[5] to the laser intensity I_L (10^{15} W/cm^2). It means that by accurately measuring the electron temperature, one is able to obtain relevant information about the value of the shock wave strength and its shot-to-shot reproducibility.

II. EXPERIMENTAL SETUP

The XFEL experimental facility at Spring-8 Angstrom Compact Free Electron Laser (SACLA),[11] Japan, was used for performing the pump–probe experiment. The pump laser was an optical Ti:Sapph laser at 800 nm wavelength, with a pulse duration of $\sim$660 ps full-width at half-maximum (FWHM) and an energy up to $\sim$1.0 J. The laser beam was focused onto a $\sim$280 μm FWHM spot, giving an on-target intensity of $\sim 2.5 \times 10^{12}$ W/cm^2 and generating a shock wave strength up to 120 GPa in different crystalline foil targets using a dedicated design to reach such high pressure. The scheme of the experiments is displayed in Fig. 1. A 7 fs XFEL pulse, with photon energies of $\sim$10.1 keV (energy bandwidth of $\sim$0.5%) and $\sim 10^{11}$ photons per pulse, was used to probe changes in the lattice spacing, *d*, of the crystalline sample. The XFEL beam irradiates the target from the rear side with respect to the optical pump laser.

The various foil targets are placed with an incident angle (typically around 20° compared to the XFEL beam axis), appropriate for diffraction measurements from the crystal lattice of the samples. The XFEL beam is focused in one axis down to $\sim$17 μm using a Kirkpatrick-Baez mirror, while the other axis is adjusted to $\sim$200 μm by a two-quadrant slit, which caused the appearance of diffraction patterns in the X-ray beam profile. Fortunately, the produced diffraction patterns were not strong enough to influence the X-ray Debye–Scherrer ring diffraction images, which were observed on a 1-megapixel array detector to retrieve the lattice spacing *d* of the sample (see Fig. 1).

The implementation of a Focusing Spectrometer with Spatial Resolution (FSSR spectrometer)[12,13] allowed us to measure the X-ray spectral intensity from the laser pump plasma and to have information about the reproducibility and the quality of the laser–solid interaction. The instrument used a spherically bent mica crystal with a lattice spacing of 2d $\sim$ 19.91 Å and a radius of curvature of R = 100 mm. We chose to use a mica crystal because it has multiple orders of reflection: 1, 2, 3, 4, 5, 7, 8, 10, 11, 12, 13. This unique property of the mica crystal is very important for using X-ray spectroscopy for characterization of laser pump plasma parameters in high energy density science experiments. Indeed, the existence of many diffraction crystal orders allowed a very wide spectral range (from practically 1 up to 19 Å) to be covered without any realignment. This meant that X-ray plasma emission from different targets could be measured using only one spectrometer. In our particular case, the crystal was aligned in such a way that in the first order of the mica crystal reflection, it was possible to record K-shell emission spectra of multi-charged Oxygen VIII lines

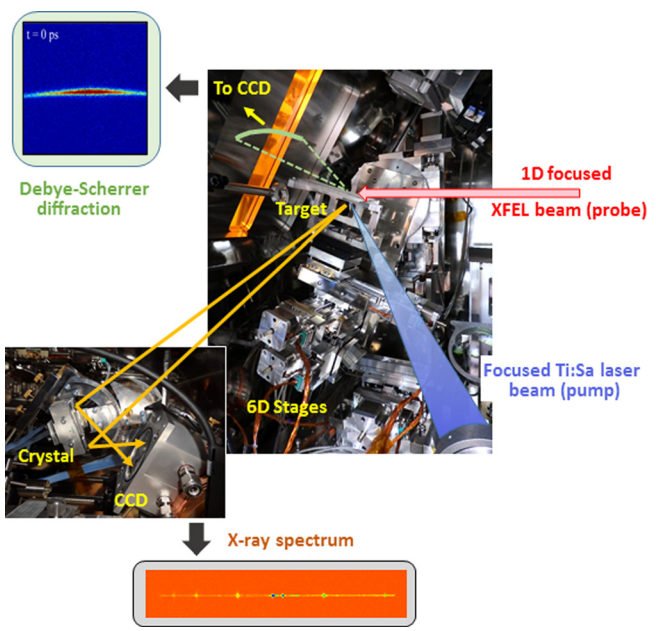

FIG. 1. Scheme of the experiments and main X-ray diagnostics. An X-ray spectrum from an Al plasma, containing lines from H-like ions of O VIII (in energy range 0.74–0.85 keV) and K-shell lines of Al (in energy range 1.48–1.7 keV) is shown at the bottom.

and Ne-like spectra of Fe XVII in the energy range of 0.735–0.84 keV. Simultaneously, the second order diffraction allowed K-shell spectra of Al and bremsstrahlung radiation of Ta spectra in the spectral range 1.47–1.68 keV to be measured. The FSSR spectral resolving power was approximately 3000 for all the measured spectra. The spectrometer observed the laser-irradiated front surface of the targets at an angle of ~40° to the target surface normal and a target-to-crystal distance of 349 mm. A vacuum compatible back-illuminated X-ray CCD Andor BN DX-440 with 13.5 μm pixel size was used for spectra registration (see Fig. 1). The X-ray CCD was protected against exposure to visible light using two layers of 1 μm thick polypropylene coated on both sides with 0.2 μm Al. This spectrometer could potentially also measure spectra at shorter wavelength ranges, but due to the low intensity of the pump laser in our experiments, the X-ray emission from the laser-produced plasma at shorter wavelengths was low and we did not measure such spectra.

Our spectrometer allowed obtaining only time integrated spectra, because the X-Ray CCD was used as a detector. In principle, it is possible to measure spectra with time resolution.[14] In such a case, it is necessary to use a streak camera as an X-ray detector Unfortunately, such detectors are expensive and time consuming to align, and consequently, it is more practical to use an X-ray CCD for pump–probe experiments. However, both the shock strength and the temperature, and therefore the X-ray spectrum, are sensitive to the highest laser intensity. We are therefore confident that the lack of time resolution does not significantly affect the capabilities of this diagnostic.

III. X-RAY SPECTROSCOPY PLASMA DIAGNOSTICS

A. Finding the best focusing position using X-ray spectra of laser plasma

The first step in our pump–probe experiments is checking the focus of the pump laser by varying the distance between the target and the focusing lens (see Fig. 2(a)). Simultaneously, the K-shell X-ray spectra of Al were measured (see Fig. 2). After target irradiation, the damages imprinted onto the Aluminium plate (see Fig. 2(b)) were checked by a microscope, and the best focal spot (which should be of the order of 50 μm) was found. The second step consists in moving the lens in the focus direction in order to be out of focus to obtain a focal spot of 280 μm FWHM, which corresponds to the laser intensity $\sim 2.5 \times 10^{12}$ W/cm^2. As can be seen in Fig. 2(c), the resulting spectra of Al plasma emission are very sensitive to the laser intensity on the surface of the target. Indeed, at large distances from the best laser focus position, the K-shell spectra of Al practically disappeared and only H-like spectra of oxygen could be observed. The observation of oxygen lines demonstrates that the FSSR used has unique sensitivity and even small impurities of oxygen, or Al target oxidation, could be detected. With better focusing of the laser beam, the incident laser intensity, and therefore the electron temperature in the plasma, increases. In such cases, the oxygen spectra practically disappeared (due to the overionization in hot plasma), and the resonance line of He-like Al ions starts to dominate. It is necessary to underline that all the presented spectra were observed in single laser shot mode. It means that results presented in Fig. 2(c) show that the proposed X-ray spectroscopic technique could be used for finding the best or appropriate focusing position *on line*, without opening the vacuum chamber and checking the damage on the laser irradiated target.

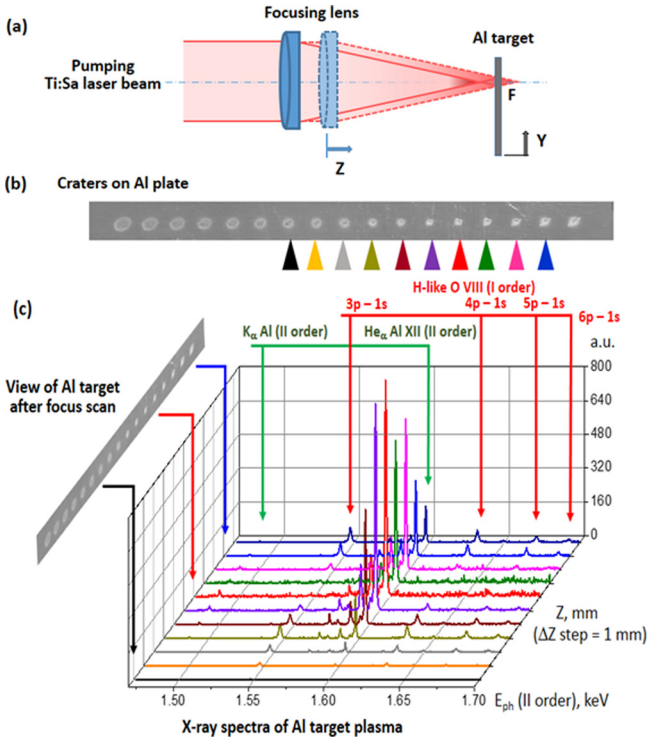

FIG. 2. (a) Scheme of experiments for checking the laser focused spots at the surface of Al plate target. (b) The images of the target irradiated by Ti:Sapph 660 ps laser and used for evaluation of the evolution of laser the spot on the target. Laser spots marked by different colors corresponding to a obtained X-ray spectra below. (c) Typical K-shell spectra of Al in second order of mica crystal reflection. Spectra of H-like O VIII were also measured in the first order of mica crystal reflection, which demonstrated the presence of impurities or oxidation in the Al foils used.

After providing the above-mentioned procedure, the pump-probe shots were carried out with Fe and Ta crystalline foil targets with various thicknesses. In each case, we observed X-ray plasma emission on the FSSR spectrometer described below. For Al and Fe plasma emission, the spectra contain mainly line radiation, while for Ta plasma due to unresolved transition arrays in multiply ionized spectra, quasi-continuum radiation dominates. Of course, the most informative are the line spectra. In such cases, we can measure both plasma density and temperature, while continuum spectra allow measurement of only the plasma temperature.

B. Diagnosing Al plasma using K spectra

Al spectra were used for the measurements of electron temperature and density of the plasma in a single laser shot on solid target laser intensity $\sim 2.5 \times 10^{12}$ W/cm^2. In the case of Al plasma, the applied spectroscopic diagnostic were based on the measurements of resonance lines of He-like Al XII ion and their dielectronic satellites' intensities.[15–17] Calculations were made using a stationary collisional-radiative kinetic model

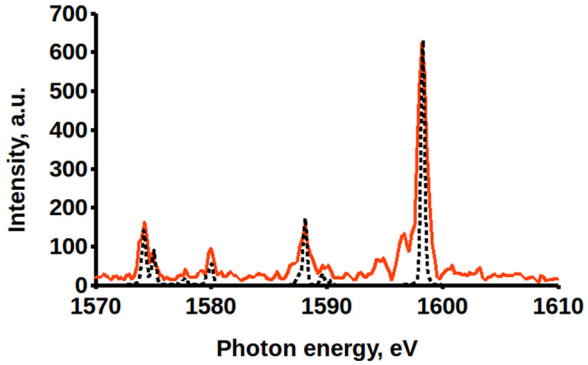

FIG. 3. (a) Red—experimentally observed K-shell Al spectra from the plasma produced by on-target laser intensity $\sim 2.5 \times 10^{12}$ W/cm^2, black dashed—simulation for $N_e = 1.3 \times 10^{20}$ cm^{-3}, $T_e = 210$ eV.

including optical thickness of the resonance lines. Comparisons of the calculated spectra with observed ones are shown in Fig. 3; the measured value of plasma densities and temperatures are shown in Table I.

C. Diagnosing Ta plasma using continuum spectra

The X-ray spectrum (bremsstrahlung radiation and quasicontinuum radiation due to unresolved transition arrays in multiply ionized Ta spectra) produced by the laser irradiation of Ta foils with 5 μm thickness has been recorded in a single shot mode. For Ta plasma, we have measured the X-ray bremsstrahlung radiation emission I_{bs} in the spectral range corresponding to photon energies from 1470 eV to 1680 eV. Because the spectral distribution $I_{bs}(E)$ exponentially depends on electron temperature $I_{bs}(E) = A\exp(-E/kT_e)$, it allows us to estimate the electron plasma temperature by the simple equation

$$d[\ln(I_{bs}(E))]/dE = -1/kT_e. \quad (3)$$

The comparisons of the observed spectrum and calculated bremsstrahlung spectra for different T_e are presented in the upper part of Fig. 4. As could be seen from such comparison, the accuracy in the determination of the electron temperature using the bremsstrahlung radiation from the Ta plasma is on the order of $\sim \pm 5\%$.

Our experiments show that the variation of Ta X-ray spectra intensities in 6 pump-probe laser shots was only of $\sim$6.4%, which implies a variation in the electron temperature of $\sim \pm 5\%$ (The highest and lowest intensity spectra are presented in Fig. 4, and the results derived from the analysis are shown in Table I). As it was mentioned in Introduction at

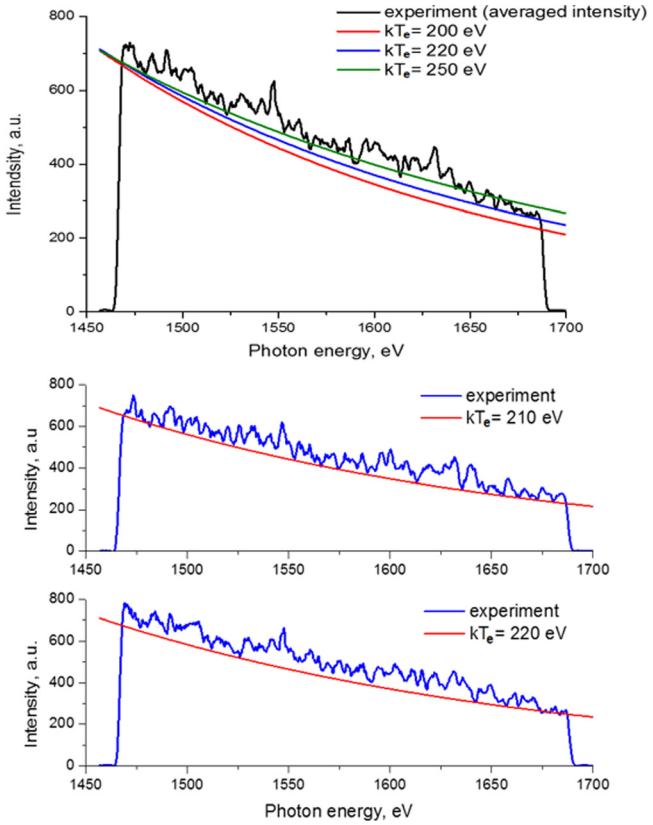

FIG. 4. Ta plasma emission in the range of 1470–1680 eV and the bremsstrahlung radiation calculated for different T_e values.

nano and sub-nanosecond duration of laser pulse and relatively low laser intensities, the electron temperature follows $T_e \sim I_L^{2/3}$. In that case, the shot-to-shot fluctuations of the laser intensities are of the order of $\sim \pm 8\%$. This value is consistent with the shot to shot RMS fluctuation ($\sim$2%) of the laser energy measured by an energy meter. According to Equation (2), shock wave strength is $P \sim I_L^{2/3}$. It means that its shot-to-shot reproducibility of P in Ta experiments was $\sim \pm 5\%$. Thus, the laser–matter interaction is very stable and can launch reproducible shot-to-shot shock wave strength inside Ta sample, which was simultaneously observed in Ref. 18 by XFEL diffraction probe measurements.

D. Diagnostic of Fe plasma using L-shell Fe spectra

In the case of Fe plasma, the spectra contain lines caused by transitions to the L-shell in Fe ions in various charge states. The modeling for the Fe L-shell emissions was done using a model that was developed to study stainless steel

TABLE I. Results of plasma diagnostics by X-ray spectroscopy methods. Equations (1) and (2) were applied to retrieve I_L and P.

Target	N_e (cm^{-3})	T_e (eV)	Laser intensity retrieved from measured T_e (W/cm^2)	Shock wave strength retrieved from measured I_L (GPa)
Ta (min)	…	210 ± 10	$3.0 \pm (0.1) \times 10^{12}$	128 ($\pm$6)
Ta (max)	…	220 ± 10	$3.2 \pm (0.1) \times 10^{12}$	133 ($\pm$6)
Fe (min)	1.2×10^{20}	220 ± 15	$3.2 \pm (0.15) \times 10^{12}$	133 ($\pm$13)
Fe (max)	0.9×10^{20}	230 ± 15	$3.4 \pm (0.15) \times 10^{12}$	140 ($\pm$13)
Al	1.3×10^{20}	210 ± 10	$3.0 \pm (0.1) \times 10^{12}$	128 ($\pm$6)

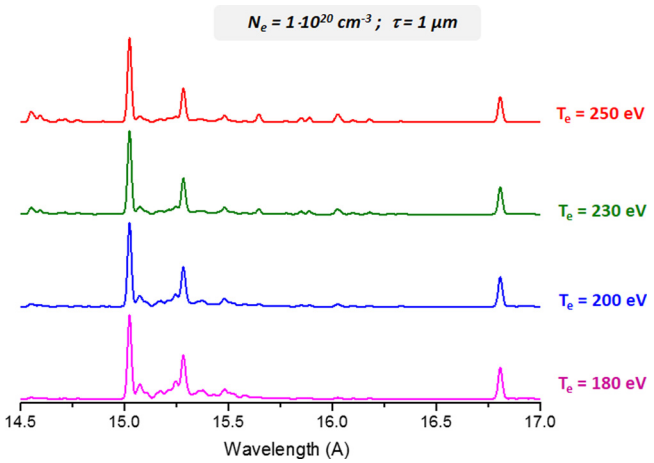

FIG. 5. Dependence of spectra intensity in the vicinity of Ne-like Fe XVII ions on electron plasma temperature.

Z-pinch wire arrays and ultrashort laser interaction with Fe solid targets.[19–21] The model used atomic data calculated by the Flexible Atomic Code (FAC).[22] Ground states for ionization levels from bare to neutral were used, while excited states for H-like to Al-like Fe ions were detailed with the largest focus being on O-like to Al-like states. For L-shell transitions, singly excited states up to $n = 5$ were used for Ne- and Na-like Fe ions, while O-, F-, Mg-, and Al-like Fe ions are included up to $n = 4$. Doubly excited states were included for Na-, Mg-, and Al-like Fe ions up to $n = 3$. The model assumes non-LTE (local thermodynamic equilibrium) conditions, and synthetic spectra are created by broadening line emissions using Voigt line profiles.

Three parameters were adjusted to match the theoretical spectrum with the experimental spectrum: electron temperature (T_e), electron density (N_e), and optical thickness (see Figs. 5 and 6). Changes to T_e were more noticeable as it is demonstrated in Fig. 5 when comparing the Ne-like lines (3C, 3D, and 3F lines of Fe in Fig. 7) with the region between 15.6 and 16.5 Å which is mostly composed of lines from F-like Fe transitions. This is due to T_e strongly affecting the ionization balance of the plasma. When matching the theory to the experiment, the T_e was adjusted to match the relative intensities of both F- and Ne-like Fe lines. The changes in N_e were more observable as shown in Fig. 6(a) when comparing the intensity of the 3C, 3D, and 3F lines. For example, increasing the N_e reduced the intensity of the 3F line relative to the 3C and 3D lines. Hence, the N_e was found in the experiments by matching the relative intensities of the 3C, 3D, and 3F lines. The optical thickness changed the intensity of all the lines by representing self absorption within the plasma. The more intense lines are typically more affected. The thickness of the plasma was determined by matching the relative intensities of the 3C and 3D lines with the structures between the two lines. The dielectronic satellite structures were not very affected by the thickness changes and therefore made good reference points to scale the 3C and 3D lines. In Fig. 7, we present comparison of the modelling results with observations. One can see a very good agreement between experiment and theory.

The accuracy in the determination of the electron temperature using the intensities of L-shell spectra in Fe plasma emission is of the order of $\sim\pm 7\%$. The variation of seven X-ray Fe spectra intensity measured in our pump–probe experiments was ~20%, which implies a variation of the electron temperature of $\sim\pm 7\%$ (see Fig. 7 and Table I). As it is mentioned earlier, with nano and sub-nanosecond duration laser pulses at relatively low laser intensities, the electron temperature goes as $T_e \sim I_{las}{}^{2/3}$. In that case, the shot-to-shot fluctuations of the laser intensities are of the order of $\sim\pm 10\%$. According to Equation (2), shock wave strength $P \sim I_L{}^{2/3}$. It means that its shot-to-shot reproducibility in Fe experiments was $\sim\pm 7\%$. The measured values of plasma parameters are shown in Table I.

IV. DISCUSSION

Table I shows that in our experiments, the stability of laser parameters such as energy, focusing laser spot reproducibility, and pulse duration was very good. The electron temperature of the plasma generated by the laser irradiation of different solids targets was in the range of $\sim 220 \pm 10$ eV, which means that the temperature deviation from the mean value for all experimental results did not exceed ± 5–7%. This suggests that the stability of the laser intensity on the target is on the order of ± 8–10%, and that therefore, the maximum amplitude of the shock wave strength propagating

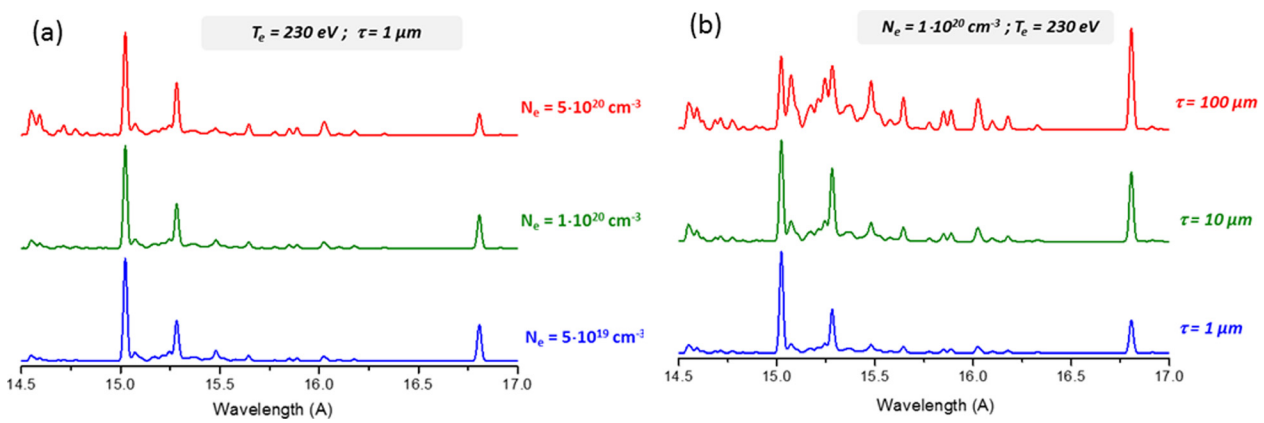

FIG. 6. Dependence of spectra intensity in the vicinity of L-shell Fe ions on electron density of plasma (a) and on plasma optical thickness (b).

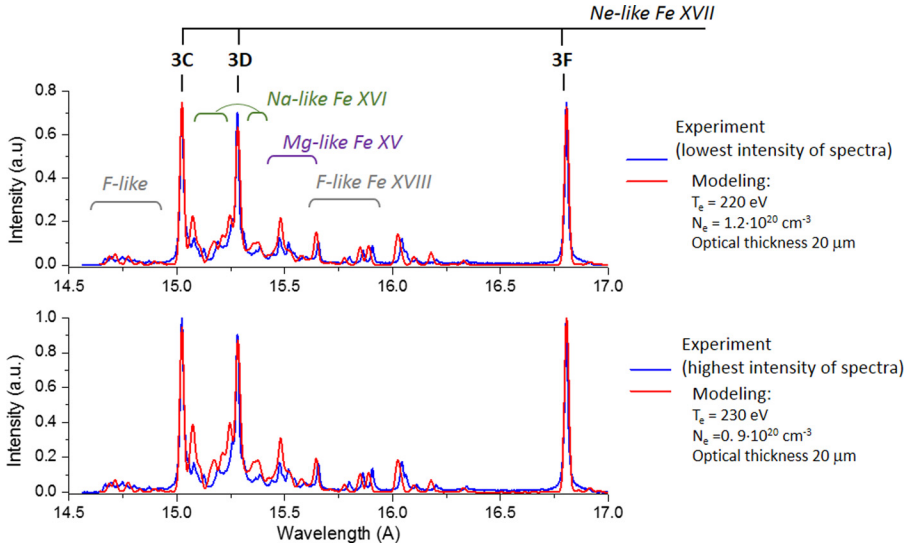

FIG. 7. Comparison of the highest and lowest emission intensity spectra of L-shell Fe plasma, obtained in a series of 7 laser pump-probe shots.

in the sample is highly shot-to-shot reproducible. Using Equation (1), we derived the laser intensity reached in our experiments as $I_l \sim 3 \times 10^{12}$ W/cm^2, which is in very good agreement with the chosen incident laser intensity. Using Equation (2), we also estimated the strength of shock waves in our experiments, which is on the order of ~130 GPa. It is necessary to mention that this value is slightly higher (116 GPa) than estimated in our pump–probe experiment, in which the dynamic fracture of Tantalum was observed at the atomic scale and compared with large scale molecular dynamics simulation.[18] This could be connected with 2 reasons: (1) We used for estimation of Te and shock wave strength Equations (1) and (2), which are valid for Z/A ratio ~0.5, whereas for the case of Ta, the ratio is 0.4. Another point is that the shock wave decays during its propagation through the target. As the diffraction diagnostic measures the shock wave at the rear side of the target compared to the optical laser beam, the estimated ablation pressure given by this spectroscopic method at the front surface of the target should be higher compared to what we measured at the rear side of the target.

We would like to stress that the reproducibility of the laser–matter interaction is of prime importance in pump-probe experiments which are dedicated, for example, to the study of phase transition in material at high pressure. Indeed, these types of experiments look at different planes of the material in order to search for new phases. In that case, it is important to control that the maximum amplitude of the shock wave is the same for the differents planes to deduce with small uncertainties the parameters of the new phase. For example, in our experimental case of Ta plasma, the variation of ±8% in the laser intensity causes a difference in the maximum amplitude of the shock wave of ~6 GPa. This is small variation that can be controlled now in order to characterize new phase parameters with high accuracy.

It is necessary to emphasise that the diagnostic presented here is not intended as an alternative to that commonly used for measuring the strength of shock waves propagating inside a material, i.e., the velocity interferometer system for any reflector (VISAR) high-precision velocity diagnostic.[23,24] Indeed, VISAR allows more direct measurements of the strength of shock waves propagating inside samples and breaking out the rear side of pumped targets. Moreover, the accuracy of VISAR measurements is higher and can be as high as few percent uncertainties on the shock velocity. However, the X-ray spectroscopic diagnostic is easier to implement in an experiment and can perform well in combination with the VISAR observation, because it gives complementary information about the laser intensity parameters on the front side of the pumped target. Simultaneous measurements by both methods will help in future experiments to obtain more accurate data in the field of shock wave generation and interaction of shock waves with different materials.

V. CONCLUSION

In this study, we present an *indirect* method to estimate the shock wave strength and allow *on line* monitoring of its reproducibility in each laser shot, even with low energy and laser intensity on the target. This method is based on a shot-to-shot measurement of the X-ray emission from the ablated plasma by a high resolution FSSR spectrometer. High sensitivity and resolved power of the spectrometer allowed spectra of Oxygen, Aluminium, Iron, and Tantalum to be obtained in laser pump-XFEL probe high energy density science experiments in each laser shot and to control fluctuations in the X-ray spectra intensity emitted by different plasmas with an accuracy of ~2%. This implies estimating the electron plasma temperature with accuracy ~±5–7%. At nano and sub-nanosecond duration of laser pulse with relatively low laser intensities, the electron temperature follows $T_e \sim I_L^{2/3}$, implying an estimation of laser intensity on the target with accuracy ~±8–10%. Knowledge of laser intensity on the target gives a chance to *indirectly* determine the laser flux on the target and to control its shot-to-shot reproducibility. Thus, it gives opportunity to monitor shock wave generation strength with high accuracy in any laser pump–probe high energy density science experiments.

ACKNOWLEDGMENTS

The XFEL experiments were performed at the BL3 of SACLA with the approval of the Japan Synchrotron Radiation Research Institute (JASRI) (Proposal No. 2015A8066). This work was supported in part by the Core-to-Core Program on International Alliance for Material Science in Extreme States with High Power Laser from the Japan Society for the Promotion of Science (JSPS), and by the X-ray Free Electron Laser Priority Strategy Program at Osaka University from the Ministry of Education, Culture, Sports, Science and Technology (MEXT, Contract No. 12005014). This work was also partly supported by Russian Foundation for Basics Research (Grant No. # 14-22-02089) and by RAS Presidium Program for basic research #11. V.Z. and N.I. acknowledge support from Russian Science Foundation (14-19-01599).

[1]R. P. Drake, *High-Energy-Density Physics: Fundamentals Inertial Fusion, and Experimental Astrophysics* (Springer, 2006).
[2]J. Colvin and J. Larsen, *Extreme Physics: Properties and Behavior of Matter at Extreme Conditions* (Cambridge University Press, 2013).
[3]V. E. Fortov, *Extreme States of Matter* (Springer, 2011).
[4]R. J. Trainor, J. W. Shaner, J. M. Auerbach, and N. C. Holmes, "Ultrahigh-pressure laser-driven shock-wave experiments in aluminium," Phys. Rev. Lett. **42**, 1154–1158 (1979).
[5]P. Mora, "Theoretical model of absorption of laser light by a plasma," Phys. Fluids **25**, 1051–1056 (1982).
[6]S. I. Anisimov, A. M. Prokhorov, and V. E. Fortov, "Application of high-power lasers to study matter at ultrahigh pressures," Sov. Phys. - Usp. **27**, 181–205 (1984).
[7]D. Batani, R. Dezulian, H. Stabile, M. Tomasini, G. Lucchini, F. Canova, R. Redaelli, M. Koenig, A. Benuzzi, H. Nishimura, Y. Ochi, J. Ullschmied, J. Skala, B. Kralikova, M. Pfeifer, T. Mocek, A. Präg, T. Hall, P. Milani, E. Barborini, and P. Piseri, "High pressure laser-generated shocks and application to EOS of carbon," J. Phys.: Conf. Ser. **71**, 012001 (2007).
[8]E. Moses, "The National Ignition Facility: An experimental platform for studying behaviour of matter under extreme conditions," Astrphys. Space Sci. **336**, 3 (2011).
[9]M. G. Gorman, R. Briggs, E. E. McBride, A. Higginbotham, B. Arnold, J. H. Eggert, D. E. Fratanduono, E. Galtier, A. E. Lazicki, H. J. Lee, H. P. Liermann, B. Nagler, A. Rothkirch, R. F. Smith, D. C. Swift, G. W. Collins, J. S. Wark, and M. I. McMahon, "Direct observation of melting in shock-compressed bismuth with femtosecond x-ray diffraction," Phys. Rev. Lett. **115**, 095701 (2015).
[10]D. Milathianaki, S. Boutet, G. J. Williams, A. Higginbotham, D. Ratner, A. E. Gleason, M. Messerschmidt, M. M. Seibert, D. C. Swift, P. Hering, J. Robinson, W. E. White, and J. S. Wark, "Femtosecond visualization of lattice dynamics in shock-compressed matter," Science **342**, 220–223 (2013).
[11]M. Yabashi, H. Tanaka, and T. Ishikawa, "Overview of the SACLA facility," J. Synchrotron Radiat. **22**(3), 477–484 (2015).
[12]A. Ya. Faenov, S. A. Pikuz, A. I. Erko, B. A. Bryunetkin, V. M. Dyakin, G. V. Ivanenkov, A. R. Mingaleev, T. A. Pikuz, V. M. Romanova, and T. A. Shelkovenko, "High-performance X-ray spectroscopic devices for plasma microsources investigations," Phys. Scr. **50**, 333–338 (1994).
[13]T. A. Pikuz, A. Ya. Faenov, S. A. Pikuz, V. M. Romanova, and T. A. Shelkovenko, "Bragg X-ray optics for imaging spectroscopy of plasma microsources," J. X-ray Sci. Technol. **5**, 323–340 (1995).
[14]P. Nickles, M. Kalashnikov, M. Shnurer, B. Bryunetkin, I. Skobelev, and A. Faenov, "High-resolution X-ray diagnostics of high-temperature plasma with picosecond time resolution," JETP Lett. **62**, 910–915 (1995).
[15]V. A. Boiko, A. Ya. Faenov, and S. A. Pikuz, "X-ray spectroscopy of multiply-charged ions from laser plasmas," J. Quant. Spectrosc. Radiat. Trans. **19**, 11–50 (1978).
[16]V. A. Boiko, A. V. Vinogradov, S. A. Pikuz, I. Yu. Skobelev, and A. Ya. Faenov, "The X-ray Spectroscopy of laser-produced plasma," J. Sov. Laser Res. **6**, 85–290 (1985).
[17]F. B. Rosmej, U. N. Funk, M. Geissel, D. H. H. Hofmann, A. Tauschwitz, A. Ya. Faenov, T. A. Pikuz, I. Yu. Skobelev, F. Flora, S. Bollanti, P. Di Lazzaro, T. Letardi, A. Grilli, L. Palladino, A. Reale, A. Scafati, L. Reale, T. Auguste, P. D'Oliveira, S. Hulin, P. Monot, A. Maksimchuk, S. A. Pikuz, D. Umstadter, M. Nanatel, R. Bock, M. Dornik, M. Stetter, S. Stoewe, V. Yakushev, M. Kulish, and N. Shilkin, "X-ray radiation from ions with K-shell vacancies," J. Quant. Spectrosc. Radiat. Transfer **65**, 477–499 (2000).
[18]B. Albertazzi, N. Ozaki, V. Zhakhovsky, A. Faenov, H. Habara, M. Harmand, N. J. Hartley, D. Ilnitsky, N. Inogamov, Y. Inubushi, T. Ishikawa, T. Katayama, M. Koenig, A. Krygier, T. Matsuoka, S. Matsuyama, E. McBride, K. Migdal, G. Morard, T. Okuchi, T. Pikuz, O. Sakata, Y. Sano, T. Sato, T. Sekine, T. Seto, K. Takahashi, H. Tanaka, K. A. Tanaka, Y. Tange, T. Togashi, K. Tono, Y. Umeda, T. Vinci, M. Yabashi, T. Yabuuchi, K. Yamauchi, and R. Kodama, "Spallation of laser-shocked tantalum lattice under extreme tensile stress recorded by X-ray real time monitoring technique," Science (submitted).
[19]A. S. Safronova, V. L. Kantsyrev, A. A. Esaulov, N. D. Ouart, U. I. Safronova, I. Shrestha, and K. M. Williamson, "X-ray spectroscopy and imaging of stainless steel X-pinches with application to astrophysics," Eur. Phys. J.: Spec. Top. **169**, 155–158 (2009).
[20]A. S. Safronova, V. L. Kantsyrev, A. A. Esaulov, N. D. Ouart, M. F. Yilmaz, K. M. Williamson, I. Shrestha, G. C. Osborne, J. B. Greenly, K. M. Chandler, R. D. McBride, D. A. Chalenski, D. A. Hammer, B. R. Kusse, and P. D. LePell, "Spectroscopy and implosion dynamics of low wire number nested arrays on the 1 MA COBRA generator," Phys. Plasmas **15**, 033302 (2008).
[21]N. D. Ouart, A. S. Safronova, A. Ya. Faenov, T. A. Pikuz, S. V. Gasilov, F. Calegari, M. Nisoli, S. De Silvestri, S. Stagira, L. Poletto, and P. Villoresi, "Analysis of the simultaneous measurements of iron K- and L-shell radiation from ultrashort laser produced plasmas," J. Phys. B: At. Mol. Opt. Phys. **44**, 065602 (2011).
[22]M. F. Gu, "The flexible atomic code," Can. J. Phys. **86**, 675–689 (2008).
[23]P. M. Celliers, D. K. Bradley, G. W. Collins, D. G. Hicks, T. R. Boehly, and W. J. Armstrong, "Line-imaging velocimeter for shock diagnostics at the OMEGA laser facility," Rev. Sci. Instrum. **75**, 4916–4929 (2004).
[24]N. Ozaki, T. Sano, M. Ikoma, K. Shigemori, T. Kimura, K. Miyanishi, T. Vinci, F. H. Ree, H. Azechi, T. Endo, Y. Hironaka, Y. Hori, A. Iwamoto, T. Kadono, H. Nagatomo, M. Nakai, T. Norimatsu, T. Okuchi, K. Otani, T. Sakaiya, K. Shimizu, A. Shiroshita, A. Sunahara, H. Takahashi, and R. Kodama, "Shock Hugoniot and temperature data for polystyrene obtained with quartz standard," Phys. Plasmas **16**, 062702 (2009).